Impact-parameter dependence of inner-shell ionization cross sections induced by protons and He ions in the energy range 0.4–2.0 MeV/u

Donald G. Simons,* David J. Land, Matt D. Brown, and C. Lewis Cocke†
Naval Surface Warfare Center, Silver Spring, Maryland 20903-5000
(Received 11 April 1990)

The impact-parameter dependence of the K-shell ionization cross section has been measured for protons and ^{3}He ions incident on thin-foil targets of Ti, Ni, and Cu at selected energies in the region from 0.4 to 2.0 MeV/u. Comparison is made of these experimentally determined values with the results of a recently developed theoretical model in which the electron binding energy and initial-state wave function are allowed to respond in a time-dependent fashion to the field of the projectile as a function of its position along a hyperbolic Coulomb trajectory. Generally good agreement between the theoretical and experimental values is obtained. A comparison between the results of this theoretical model and two other published theoretical results and with experimental data for 0.5-MeV p in Cu is also shown. Remarkably close agreement is seen, particularly between the predictions of the rather disparate theoretical models. Measurements for a single system, 2.0-MeV p in Sm, involving ionization from the L shell, are also reported.

I. INTRODUCTION

After many years of experimental investigation, there has begun to emerge some fairly extensive data sets[1] for the total K-shell ionization cross section induced by protons and helium ions for many low- to medium-Z targets at low to moderate velocities, leading to some modest understanding of the process. There is generally good agreement between theoretical and experimental values of the total cross section for incident protons.[2,3] However, an increasingly larger discrepancy which is observed for heavier projectiles such as helium and lithium ions suggests that current theoretical descriptions are not yet complete.[2,4] In order to clarify the overall picture, more detailed experimental measurements such as those pertaining to differential cross sections could be helpful.

The present paper reports results of new experimental measurements of the impact parameter dependence of the K-shell vacancy production cross section for incident protons and helium ions in elemental thin-foil targets of Ti, Ni, and Cu at selected energies from 0.4 to 2.0 MeV/u. These are cross sections differential in the projectile scattering angle. Also reported is the result of a measurement of a single system involving L-shell vacancy production, that of 2.0-MeV p in Sm. This paper is part of a mutually interactive experimental-theoretical program at the Naval Surface Warfare Center (NSWC) whose goal is to increase the data base, and to enhance the understanding of inelastic atomic collision processes and, in particular, of the most fundamental interaction leading to inner-shell ionization. The measurements were performed at the NSWC 2.5-MV Van de Graaff accelerator. In previous papers[5,6] the results of measurements of the total K-shell ionization cross section induced by protons and helium ions on selected targets from Sc through Ag in the energy region of 0.2 to 2.5 MeV/u were presented. The projectile-target-energy parameters considered in those investigations of the total cross section include the parameters studied here so that reliable values for the total cross section are available to normalize the ionization probabilities as a function of impact parameter. In a separate paper[2] a theoretical model, in which the initial-state electron binding energy and wave function are taken to be time dependent, is developed. The temporal dependence is determined from the response of the electron to the position of the projectile on a hyperbolic, Coulomb trajectory. Comparison of the results of calculations for the impact parameter dependence performed within this model with the present experimental data and with other data will be shown.

II. EXPERIMENTAL PROCEDURES

The impact-parameter dependence of the K-shell vacancy production is determined from the coincidence rate between x rays induced by particles scattered through a fixed angle θ and the scattered particle. Assuming single-event scattering, the scattering angle defines the impact parameter b within the context of the semiclassical approximation. The coincidence rate C is given by

$$C = N_p(b) P(b) \omega_k \xi_x d\Omega_x ,$$

where $N_p(b)$ is the scattered particle rate for particles scattered at the angle θ, $P(b)$ the impact parameter dependence for K-shell vacancy production probabilities, ω_k the x-ray fluorescence yield for K-shell vacancies, ξ_x the x-ray detector efficiency, and $d\Omega_x$ the x-ray detector solid angle. For the scattering angles covered in this study the relationship between the scattering angle θ and the impact parameter b is approximated by

$$b = \frac{Z_P Z_T e^2}{E\theta} ,$$

where Z_P and Z_T are the atomic numbers of the projec-

tile and the target atoms, respectively, e the electronic charge, and E the projectile energy.

In order to increase the probability for measuring a coincidence, a large x-ray detector solid angle is needed. This necessity makes it difficult to measure the solid angle directly since small errors in detector distance or aperture diameter can make appreciable differences in the measured solid angle. Instead, the product of the fluorescence yield, the detector efficiency, and the x-ray detector solid angle $\omega_k \xi_x d\Omega_x$ is determined from the simultaneous measurement of the x-ray production with particles Rutherford scattered into a monitor particle detector placed at an angle ψ. By this simultaneous measurement the need to measure the beam current and the target thickness is also eliminated. This product is the effective x-ray detector efficiency and is given by

$$\omega_k \xi_k d\Omega_x = \frac{N_x d\sigma^R(\psi,E)/d\Omega d\Omega_p(\psi)}{N_p(\psi)\sigma_T(E)} ,$$

where N_x is the x-ray detector count rate, $N_p(\psi)$ the monitor particle detector count rate, $d\sigma^R(\psi,E)/d\Omega$ the Rutherford scattering cross section at the monitor particle scattering angle ψ and energy E, $d\Omega_p(\psi)$ the monitor particle detector solid angle, and $\sigma_T(E)$ the total K-shell vacancy production cross section. We note that an accurate measurement of the total vacancy production cross section must be made independently of this experiment. However, only a single measurement at a single energy for each target element need be made. For instance, the determination of $\omega_k \xi_x d\Omega_x$ from 2-MeV protons on Cu is not only sufficient for protons on Cu at all other energies but for any other projectile on Cu provided the geometry for the x-ray detector is not changed.

The experimental setup is shown schematically in Fig. 1. The x-ray detector, a Si(Li) detector with a 190-eV resolution for ^{55}Fe x rays, is mounted at 90° with respect to the beam. It is placed as close to the target as possible without endangering its 1-mm Be window. A 0.1-mm polyethylene absorber is also placed in front of this detector to prevent scattered ions from entering the detector and causing radiation damage. Coincidence events between the x-ray detector are measured using standard techniques with the respective detector pulses triggering the start and stop inputs of a time-to-amplitude converter (TAC) spectrometer. The impact-parameter scattering angle is obtained by placing an angular aperture in front of the in-line detector and changing the distance between the aperture-detector and the target. Angular selection between 0.5° and 10° is easily obtained using this arrangement. Simultaneous measurements for two scattering angles are made possible by using a double annular aperture arrangement as shown in Fig. 2. The diameters of the two apertures are 0.80 and 0.59 cm. The method for detector alignment along the beam axis and for differentiation between particles scattered into the two angles will be described below.

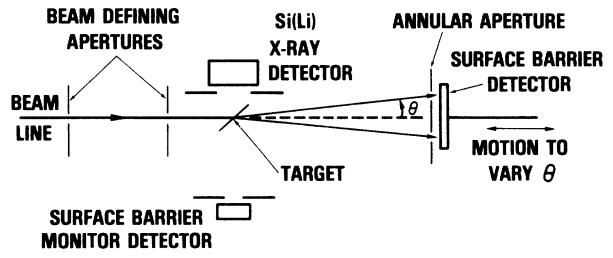

FIG. 1. Schematic of the experimental arrangement to determine the impact-parameter dependence of particle-induced K-shell ionization. The scattering angle is changed by varying the distance between the target and the downstream annular aperture. The apparent x-ray detector efficiency is determined through simultaneous monitor particle and x-ray detector measurements.

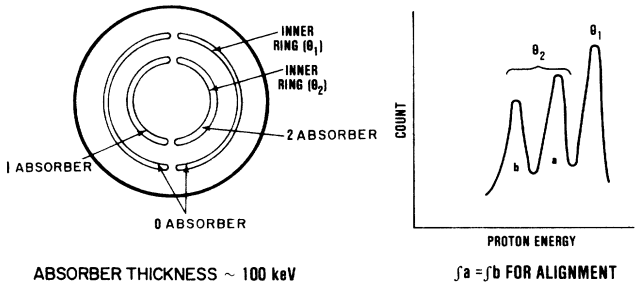

FIG. 2. Detail of the double annular aperture for simultaneous measurements at two scattering angles showing a representative particle spectrum. Covering the inner annulus with thin-foil energy absorbers allows differentiation of particles scattered into the two apertures. In addition, a means of beam alignment is provided by transverse motion of the aperture-detector system such that the average number of particles scattered into both halves of the inner annulus is equal.

The monitor particle detector is placed at 90° to the beam and opposite to the x-ray detector. This detector is a Si surface barrier detector and subtends a solid angle of 2.07×10^{-3} sr. The solid angle for the monitor detector is measured both geometrically and with calibrated radioactive sources of ^{241}Am and ^{148}Gd. Agreement between solid angles determined by the two methods is within experimental error.

Beam definition is obtained with two apertures 82.5 cm apart upstream from the target. The aperture diameters are selected such that the half-angle beam divergence is 0.43 mrad for the proton beam and 0.90 mrad for ^{3}He. With either set of apertures the beam spot at the position of the annular aperture is no more than $\frac{1}{10}$ of the diameter of the smaller annular aperture. A 2.5-mm cleaning aperture is placed between the two beam-defining apertures to minimize the split edge scattering.

A. Beam alignment and scattering angle differentiation

Prior to a measurement at any set of double angles it is necessary to align the center of the annular aperture onto the beam line. It is also necessary to provide a means to identify the particles scattered into each annular aperture. These two necessities are accomplished as follows. The inner annulus is covered with thin foils which attenuate the beam energy by approximately 100 keV per

foil thickness and reduce the apparent energy of those particles scattered at the smaller angle. In particular, the foils are arranged such that a single foil thickness covers one half of the annulus and a double foil thickness covers the other half. Thus, as shown in Fig. 2 a typical spectrum of the scattered particles consists of three energy peaks. The highest energy peak results from scattering into the larger aperture which has no absorber and defines particles scattered at the larger of the two angles. The lower two energy peaks result from particles scattered into the smaller angular aperture and defines particles scattered at the smaller of the two angles with each energy peak identifying particles scattered into each half of the smaller aperture. Alignment is accomplished by moving the aperture-detector system transverse to the beam line so that the total number of counts from particles entering each half of the inner annulus are equal. In order to compensate for the possibility of unequal size in each half of the inner annulus, the detector–double-aperture arrangement is rotated through 90° increments and the counts appropriately averaged. Alignment is achieved when the average counts through the single and double absorbers are equal. Alignment of the center of the double apertures to the beam line is accomplished to better than ± 0.05 mm by this procedure.

B. Electronic arrangements

Standard techniques are used for the coincidence measurements between the scattered particles and the emitted x rays. Since simultaneous measurements are made for two scattering angles, two time–to–pulse-height converters are used. Each is started by the x-ray signal and stopped by the appropriate energy-analyzed particle signal which defines the proper scattering angle. The TAC outputs were also strobed by the x-ray signal of the proper energy to ensure that only K-shell x rays are analyzed. The output spectra are analyzed for both true coincidences and accidental coincidences, the latter being obtained from the "flat" part of the TAC spectra. In order to determine if consideration of beam current fluctuations are needed when determining the accidental coincidence rate, a time–to–pulse-height measurement at high beam currents is made between the monitor detector and the x-ray detector, a condition for which true coincidences would be insignificant. No significant fluctuations are observed. The full width at half maximum (FWHM) resolution of the TAC spectra for true coincidences is of the order of 15 nsec.

C. Corrections to the data

It is necessary to make corrections to the data in order to compensate for spurious particle detector counts which have a negligible probability of producing an x ray. The most important of these is due to the multiple scattering at small scattering angles. These particles are assumed to produce not more than one inner shell vacancy. Tables from Sigmund and Winterbon[7] are used to determine the multiple scattering correction factor as a function of target thickness, beam energy and scattering angle. Target thicknesses are chosen such that this correction factor is no larger than 25% for any scattering angle. Corrections to the particle count are also made for slit-edge scattering and from the carbon substrates. Finally, a correction is made to the particle rate so that the quoted beam energy is that which the beam attains when it reaches the center of the target.

III. RESULTS

The impact-parameter dependence of K-shell vacancy production probabilities $P(b)$ has been measured for protons and ^{3}He projectiles incident on Ti, Ni, and Cu. In Table I we list the energies and the target thicknesses used. Target thicknesses were measured by Rutherford backscatter spectroscopy using 2.0-MeV ^{4}He ions. The results of the measurements of $P(b)$ are given in Fig. 3. The errors in the data points come from two sources: uncertainty arising from the counting statistics and uncertainty arising from the error in the multiple scattering correction due to a 10% uncertainty in the target thickness. These errors are added in quadrature. Also shown in the plots for each collision system are the target K-shell radius $R_K = a_0/(Z_T - 0.3)$, where a_0 is the Bohr radius and Z_T is the target atomic number, and the adiabatic radius $R_{ad} = (\hbar v/E_B)R_K$, where v is the projectile velocity and E_B is the K-shell electron binding energy.

The curves in the figure are obtained from a theoretical model of Land, denoted by PBBCDP and described in detail elsewhere.[2,8,9] [PBBCDP is a pseudoacronym, PB standing for $P(b)$, the probability for ionization at impact parameter b, B for binding, C for Coulomb trajectory, and DP for (dipole) polarization.] In this model the effects of the temporally varying distortions, arising from the change of the binding energy and polarization of the K-shell electron is induced by the passing projectile, are accounted explicitly. The model may be summarized by noting the expression for the scattering amplitude $b_{fi}(\infty)$:

$$b_{fi}(\infty) = -i \int_{-\infty}^{\infty} dt \exp\left[i \int_0^t dt' [H_{ff}(t') - H_{ii}(t')] \right] \times (\phi_f, V(t)\Psi_{pol}(\mathbf{R}(t))) \, . \quad (1)$$

Here $V(t)$ is the Coulomb potential between the projectile having atomic number Z_P and the target electron $V(t) = e^2 Z_P/|\mathbf{r} - \mathbf{R}(t)|$ plus a term to include target recoil. $\Psi_{pol}(\mathbf{R}(t))$ is an initial-state wave function which

TABLE I. Projectiles, energies, targets, and nominal target thicknesses used for impact parameter dependence of K-shell vacancy production probability measurements.

Projectile	Energy (MeV)	Target	Thickness (Å)
Proton	2.0	Cu	500
Proton	2.0	Ni	500
Proton	2.0	Ti	250[a]
Proton	1.0	Ti	250[a]
^{3}He	3.0	Cu	500
^{3}He	3.0	Ti	1000[a]
^{3}He	3.0	Ti	250[a]
^{3}He	1.2	Ti	250[a]

[a]Target supported on 2.7 μg/cm^2 carbon

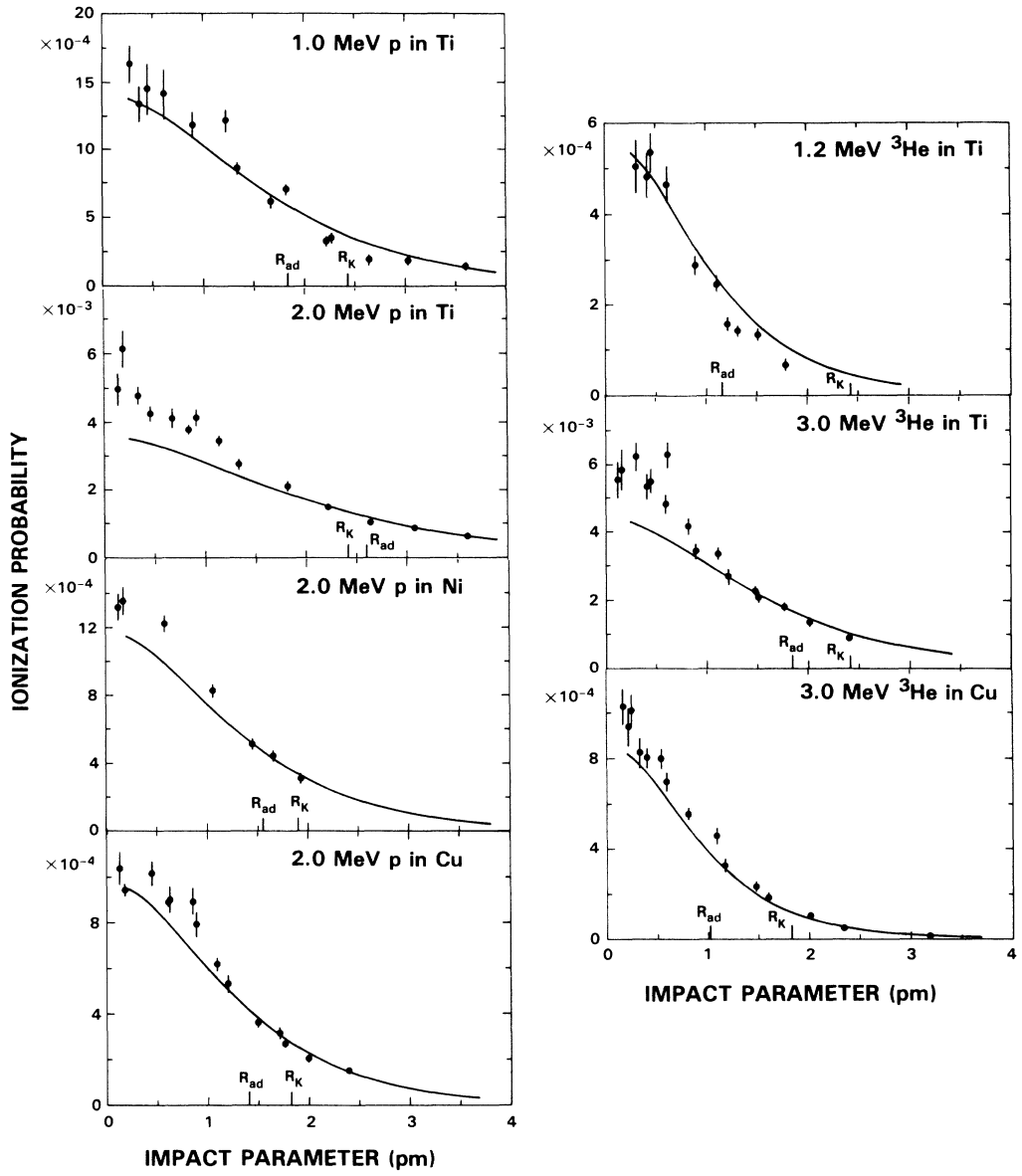

FIG. 3. Values of the K-shell ionization probability as a function of impact parameter as measured experimentally in the present work (solid circles with error bars) and as calculated theoretically with the PBBCDP model (Ref. 2) (solid curves), for each of the systems investigated here. The adiabatic radius R_{ad} and the K-shell radius R_K are shown in each plot.

describes the response of the electronic cloud, a distortion or polarization, to the motion of projectile having trajectory $\mathbf{R}(t)$. ϕ_f is the final-state wave function describing the ejected electron, taken to be a continuum Coulomb eigenfunction of the atomic Hamiltonian H_a. $H_{ii}(t)$ and $H_{ff}(t)$ are diagonal matrix of the total time-dependent Hamiltonian $H(t)=H_a+V(t)$. $\mathbf{r}$ is the electron coordinate. A hyperbolic trajectory is used to describe the motion of the projectile $\mathbf{R}(t)$ in the Coulomb field of the target nucleus with target recoil included. Other physical effects, well known to influence the K-shell ionization probability, are estimated from the energy-loss perturbed-stationary-state relativistic (ECPSSR) model of Brandt and Lapicki.[10] There is generally fairly close agreement between experimental points and the theoretical curves, with differences occurring in some cases at the smaller values of impact parameter.

It is of interest to compare the results of this theoretical model for $P(b)$ with other theoretical results and with other experimental data. This comparison is done in Fig. 4 for 0.5-MeV protons incident on Cu, in which we show recent results of Mukoyama and Lin[11] and the results of coupled channel calculations of Reading *et al.*[12] The experimental data are from Andersen *et al.*[13] The theoretical results are in good agreement with the data but, most remarkably, are very close to each other despite the fact that the details of the calculations are quite different. The coupled-channel calculations are intended as an ex-

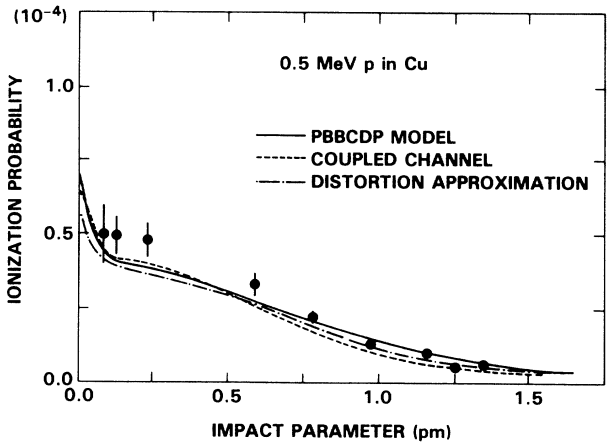

FIG. 4. Comparisons of the K-shell ionization probability as a function of impact parameter for 0.5-MeV p in Cu for the PBBCDP model involving time-dependent binding and polarization[2] (solid line), the couled-channel calculations (Ref. 12) (dashed line), and the distortion approximation (Ref. 11) (dash-dotted) line. The experimental points (solid circles with error bars) are from Ref. 13.

act solution of the Schrödinger equation for the direct Coulomb interaction between projectile and target electron in the independent-particle model. A pseudostate description of the unperturbed basis states is employed. The model of Mukoyama and Lin utilizes the distortion approximation proposed by Bates.[14] The scattering amplitude is similar to that of Eq. (1), except that an unperturbed initial-state wave function is used instead of the polarized wave function $\Psi_{\rm pol}(t)$. A pseudostate description is used here also. The incorporation of polarization is well known for giving rise to an increase in the cross section for K-shell ionization,[15] and this point clearly constitutes a difference between the distortion approximation and the PBBCDP model. However, the use of pseudostates in Ref. 11 vis-à-vis the use of continuum Coulomb wave functions in the PBBCDP model also marks a significant difference. In the case of the continuum Coulomb states, it was argued[8] that the diagonal matrix elements V_{ff} are zero in the present context of electron excitation to a continuum final state (ionization). However, diagonal matrix elements of the interaction potential with respect to continuum pseusostates V_{ff} are not zero and their presence in the exponential term in the scattering amplitude, Eq. (1), serves to offset partially the effect of the increased electron binding energy, described by the term $V_{ii}(t)$, which is well known to decrease the cross section. Hence, the net effect of the use of pseudostates is to increase the cross section over what would be obtained through the use of continuum Coulomb states. The two effects, that of employing a polarized wave function and that of employing pseudostates for continuum states, appear to compensate one another as the corresponding ionization production probabilities are seen to be very close. It should be noted that energy loss and relativistic effects are not included in the PBBCDP model in this comparison because these effects are not incorporated in the other two calculations.

Some additional assessment of the validity of the PBBCDP theoretical results for the K-shell ionization probabilities can be inferred from a consideration of the total K-shell ionization cross section. In Table II comparisons between values of the total cross section experimentally measured at the NSWC and the results of calculations based upon the PBBCDP theoretical model are given for the systems studied here. There is generally good consistency between the two. The PBBCDP theoretical results are very close for 2-MeV p in Ni or Cu but are low by as much as 16% for 3-MeV ^{3}He in Ti. Generally close agreement with the theoretical results of the PBBCDP model was found for the results of all measurements of the total cross section for incident protons with systematic discrepancies observed for incident ^{3}He. Detailed discussion of these comparisons is given elsewhere.[2] It would appear that three of the four systems with the lowest percentage difference (see Table II) in the total cross section from theory exhibit the largest discrepancies in the vacancy production probabilities at small impact parameter. However, there is also some

TABLE II. Values of the experimental and PBBCDP theoretical total K-shell ionization cross sections $\sigma^{\rm expt}$ and $\sigma^{\rm theor}$ corresponding to the cases studied in this work and percentage difference between the two. Also shown for comparison are the values of the total cross section predicted by the ECPSSR model (Ref. 10) $\sigma^{\rm ECSPPR}$, and the reference cross section developed by Paul and Muir (Ref. 1) for incident protons $\sigma^{\rm ref}$. Values for the quantity κ, which is defined in the text and which must be much greater than unity for the semiclassical approximation to hold, are noted. All cross sections are given in barns.

Target	Projectile	Energy (MeV)	κ	$\sigma^{\rm expt}$ (b)	$\sigma^{\rm theor}$ (b)	diff (%)	$\sigma^{\rm ECPSSR}$ (b)	$\sigma^{\rm ref}$ (b)
Ti	p	1.000	6.95	228	222	3	241	233[b]
		2.000	5.92	921	861	6	942	934
	^{3}He	1.206[a]	21.92	41.9	37.9	9	45.1	
		3.015[a]	13.85	787	658	16	809	
Ni	p	2.000	6.26	128	127	1	134	130[b]
Cu	p	2.000	6.48	94.3	93.2	1	98.8	95.7[b]
	^{3}He	3.015[a]	18.26	49.0	46.3	5	52.0	

[a]Values correspond to 0.4 and 1.0 MeV/u, respectively, the actual energies of the measurements of the total cross sections.
[b]Values used for the determination of the product $\omega_k \xi_x d\Omega_x$.

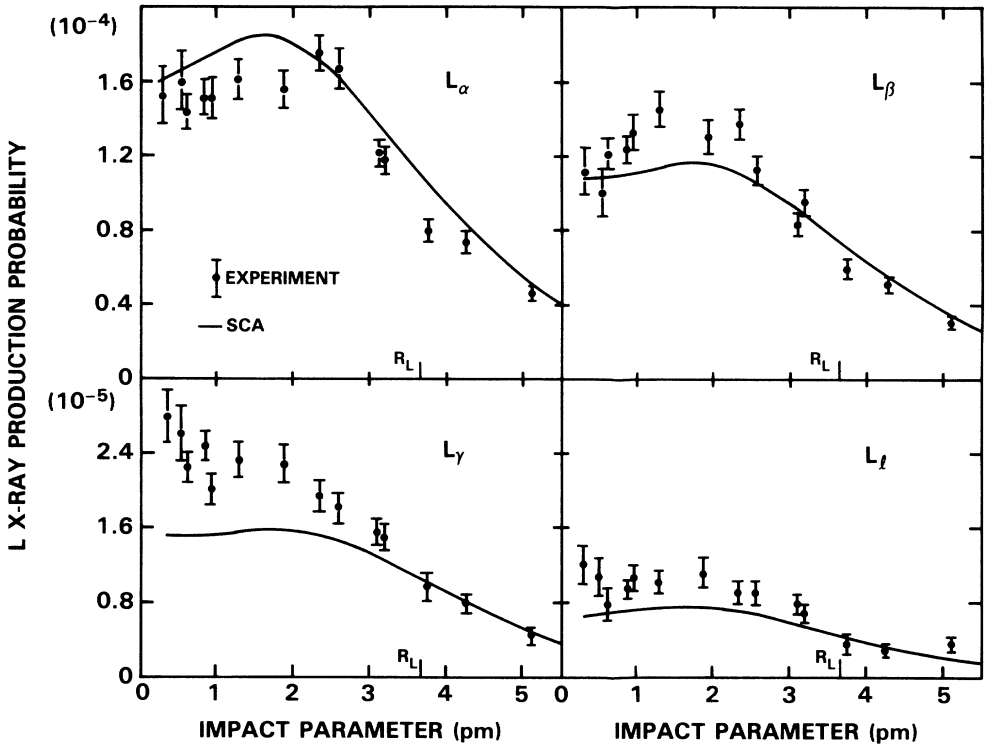

FIG. 5. Measured values of the L x-ray production probability for the $L\alpha$, $L\beta$, $L\gamma$, and Ll lines as a function of impact parameter for 2.0-MeV p in Sm. The solid curves are based on the semiclassical approximation of Ref. 17. The adiabatic radii, with values of 3.33, 3.53,nd 3.84 pm for the $L_{\rm I}$, $L_{\rm II}$, and $L_{\rm III}$ subshells, respectively, as close to the L-shell radius R_L which is shown.

discrepancy for the cases of 2-MeV p in Ni and Cu for which very close agreement is found for total cross sections. Also shown in the table are the predictions of the ECPSSR model[10] and the reference cross section for incident protons developed by Paul and Muir[1] and based upon a systematic average of many experimental measurements. Detailed discussion of the comparison of these values with experiment is also given elsewhere.[6] The comparisons between theoretical results and experimental measurements presented here might suggest that this theory satisfactorily explains the data for the parameter region in projectile and target atom and energy studied here. However, a broader overview[2] hints that the close agreement for protons may be somewhat fortuitous and that further elaboration of the theoretical modelling related to K-shell ionization is required.

One other quantity listed in Table II is the variable κ, defined as the ratio of the distance of closest approach of the projectile to the target nucleus $2d$ to the deBroglie wavelength of the projectile λ. The condition that this quantity be much greater than unity,

$$\kappa = 2d/\lambda \gg 1 ,$$

must be met in order that the semiclassical approximation hold.[16] It is only within this approximation that the relation between the impact parameter b and the projectile scattering angle θ noted above is established. It is clear from the table that this condition is satisfactorily met, particularly for the cases involving incident He.

Our results for the single case we have studied of ionization from the L shell, 2.0-MeV p in Sm, are presented in Fig. 5. Here are shown our experimental measurements of the L x-ray production probability versus impact parameter for the $L\alpha$, $L\beta$, $L\gamma$, and Ll x rays. The solid curves are the results of theoretical calculations employing the semiclassical approximation in lowest-order perturbation theory[16] for the $L_{\rm I}$, $L_{\rm II}$, and $L_{\rm III}$ subshell ionization cross sections from tables of Hansteen *et al.*[17] The L x-ray production probabilities were constructed with the use of the fluorescence yields and Coster-Kronig factors of Ref. 18 and the radiative yields of Ref. 19. The overall agreement is quite satisfactory. In particular, the close correspondence in the shape of the curves for the $L\alpha$ and $L\beta$ lines is noteworthy.

IV. CONCLUSIONS

Measurements of the impact parameter dependence of the K-shell vacancy production probability have been made for seven systems involving incident protons or ^{3}He ions. Good agreement is found with a theoretical model in which explicit time dependence of the K-shell binding energy and wave function is taken into account. Surprisingly close agreement is found between three different theoretical models and with experimental data for the

case of 0.5-MeV protons incident on copper. Measurements were also reported for a single case involving vacancy production from the L shell; satisfactory agreement is obtained with calculations based on the semiclassical approximation in lowest-order theory in terms of the L x-ray production probability for the $L\alpha$, $L\beta$, $L\gamma$, and Ll lines. Despite the close agreement between the experimental data and the results of a theoretical model shown here, a larger overview of total cross sections for incident He and Li ions suggests that additional interaction beyond the direct Coulomb interaction is required.

ACKNOWLEDGMENTS

The authors wish to thank Mr. Patrick K. Cady for his tireless efforts in the data acquisition. This work was supported by the Independent Research Program of the Naval Surface Warfare Center.

---

*Present address: Catholic University of America, Washington, D.C. 20064.

†Permanent address: Kansas State University, Manhattan, KS 66506.

[1]H. Paul and J. Muir, Phys. Rep. **135**, 47 (1986).

[2]D. J. Land (unpublished).

[3]J. M. Hansteen, L. Kocbach, and A. Graue, Phys. Scr. **31**, 63 (1985).

[4]D. J. Land, Nucl. Instrum. Methods A **240**, 470 (1985).

[5]M. D. Brown, D. G. Simons, D. J. Land, and J. G. Brennan, Phys. Rev. A **25**, 2935 (1982).

[6]D. G. Simons, J. L. Price, D. J. Land, and M. D. Brown, Phys. Rev. A **39**, 3884 (1989).

[7]P. Sigmund and K. B. Winterbon, Nucl. Instrum. Methods **119**, 541 (1974).

[8]D. J. Land, Nucl. Instrum. Methods B **27**, 491 (1987).

[9]D. J. Land, Nucl. Instrum. Methods B **42**, 436 (1989).

[10]W. Brandt and G. Lapicki, Phys. Rev. A **23**, 1717 (1981).

[11]T. Mukoyama and C. D. Lin, Phys. Rev. A **40**, 6886 (1989).

[12]J. F. Reading, A. L. Ford, M. Martir, and R. L. Becker, Nucl. Instrum. Methods **192**, 1 (1982).

[13]J. U. Andersen, E. Laegsgaard, and M. Lund, Nucl. Instrum. Methods **192**, 79 (1982); E. Laegsgaard (private communication).

[14]D. R. Bates, Proc. R. Soc. London **73**, 227 (1959).

[15]G. Basbas, W. Brandt, and R. Laubert, Phys. Rev. A **17**, 1655 (1978).

[16]J. Bang and J. M. Hansteen, K. Dan. Vidensk, Selsk. Mat.—Fys. Medd. **31**, No. 13 (1959).

[17]J. M. Hansteen, O. M. Johnsen, and L. Kocbach, At. Data Nucl. Data Tables **15**, 305 (1975).

[18]E. J. McGuire, Phys. Rev. A **3**, 587 (1971).

[19]J. H. Scofield, Phys. Rev. **179**, 9 (1969).